Benchmarking Control Techniques Applied to Magnetic Bearings: Performance Assessment Criteria Analysis

José Dalvio Ghirello Garcia[1,a], Afonso Celso del Nero Gomes[2,b], Richard Magdalena Stephan[2,c]

[1]Instituto Federal de Educação, Ciência e Tecnologia do Rio de Janeiro(IFRJ)
Rua Lúcio Tavares, 1045, Nilópolis/RJ, Brazil
[2]Departamento de Engenharia Elétrica, COPPE/EE/UFRJ
Caixa Postal 68504, Rio de Janeiro/RJ, Brazil
[a]jose.garcia@ifrj.edu.br, [b]nero@coep.ufrj.br, [c]richard@coe.ufrj.br

Abstract: Active Magnetic Bearings, due to a plant-intrinsic instability, require a control system for normal operation. Many control strategies have been proposed for the stabilization task, in some instances emphasizing market recognized control approaches, as PID controllers arranged in decentralized structures, and in other instances modern control approaches are envisaged, like LQR or H∞ structures. The objective of this paper is to present criteria to assess the performance of such proposed controllers, in order to establish a metric to compare different control schemes. The performance assessment criteria discussed include time domain as well as frequency domain approaches. Such criteria are applied to two control systems used in a laboratory prototype to stabilize a bearingless motor, being one based on PID controllers and the other being a LQR scheme. Discussion of the results is used to select a metric to be applied in the comparison of some controller algorithms, both centralized and decoupled, in order to determine which control law best suits such a bearingless motor.

Keywords: Active Magnetic Bearing, Bearingless Motors, Controller Performance Assessment, Performance Criteria

Introduction

Magnetic bearings, being intrinsically unstable, have been made feasible with the usage of control systems. Many different control schemes have been proposed [1, 2, 3, 4, 5]. In some instances, the evaluation of the control loop performance has been based on traditional indexes, like step response. Nevertheless, magnetic bearings have a scope which require, more than anything, that a central position be maintained no matter what disturbances are likely to be applied. It is recognized that there is not a unique optimal approach to such a control problem, but the best approach for the specific plant dynamic under consideration. To address this performance assessment problem, a criteria that allows for a better benchmarking of the different control approaches applied to a specific plant was reached.

Among the various approaches found in literature for performance assessment, two are selected for analysis, in order to be applied to the problem of benchmarking controllers used in a bearingless induction motor. Firstly, the basic theory of stochastic performance assessment is discussed, based on the work of [6] and [7]. A frequency domain approach is briefly discussed, as presented by [8].

Performance Assessment Criteria

Controller performance assessment is a discipline that has been explored mainly by the area of process control, and has produced different criteria to monitor and evaluate control loop

performance. Qin [6] presented various techniques that appear in recent literature, and has explored a method of his own; this review of criteria presents both minimum variance based algorithms, as well as frequency domain approaches. In the following sections, stochastic performance evaluation and frequency domain analysis are briefed.

Stochastic Performance Assessment. Consider the control structure shown in Figure 1. By inspection, the following development applies:

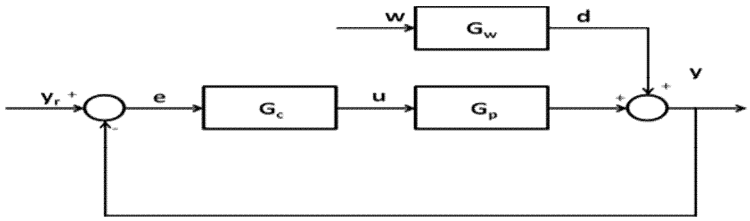

Figure 1 Control structure

$$y(k) = \frac{B_p(z^{-1})z^{-b}}{A_p(z^{-1})}\,u(k) + d(k). \qquad (1)$$

$$d(k) = \frac{B_w(z^{-1})}{(1-z^{-1})A_w(z^{-1})}\,w(k). \qquad (2)$$

$$u(k) = -G_c(z^{-1})(y(k) - y_r). \qquad (3)$$

Assuming that polynomials A_p, B_p, A_w and B_w are stable, meaning that they have their roots inside the unit circle [6], and letting $y_r = 0$, then the following expressions may be written:

$$y(k) = \frac{B_p(z^{-1})z^{-b}}{A_p(z^{-1})}\left(-G_c(z^{-1})y(k)\right) + d(k). \qquad (4)$$

$$y(k) = \frac{d(k)}{1 + \frac{B_p(z^{-1})z^{-b}}{A_p(z^{-1})}G_c(z^{-1})}. \qquad (5)$$

Finally

$$y(k) = \frac{\frac{B_w(z^{-1})}{(1-z^{-1})A_w(z^{-1})}}{1 + \frac{B_p(z^{-1})z^{-b}}{A_p(z^{-1})}G_c(z^{-1})}\,w(k) = \frac{B_{cl}(z^{-1})}{A_{cl}(z^{-1})}. \qquad (6)$$

By long division, y(k) may be expressed as

$$y(k) = \frac{B_{cl}(z^{-1})}{A_{cl}(z^{-1})} = \left(1 + \psi_1 z^{-1} + \psi_2 z^{-2} + \cdots + \psi_{b-1}z^{-(b-1)} + \psi_b z^{-b} + \cdots\right)w(k). \qquad (7)$$

According to [7], this series converges if closed loop system is stable, and this expansion is valid for the computation of impulse weights ψ_i. The first b-1 weights ψ_i are equal to the b-1 coefficients of the impulse response of the disturbance transfer function and are not

affected by any controller been applied to the plant. The net result is that, under minimum variance controller, the system output variance is given by:

$$\sigma_y^2 = \sigma_{MV}^2 = \left(1 + \psi_1^2 + \psi_2^2 + \cdots + \psi_{b-1}^2\right)\sigma_w^2. \quad (8)$$

Those results lead to the following performance assessment evaluation algorithm using plant output data [6]:

1. Estimate process delay *b*.
2. Identify closed loop model, relating plant output to noise *w*. An ARMA model is suggested for this purpose.
3. Obtain impulse response b*y* considering the leading *b-1* coefficients of
   $y(k) = w(k) + \sum_1^{b-1} \psi_i\, w(k-i) + \text{remainder}$
4. Calculate minimum variance estimate, given by
   $\sigma_{MV}^2 = (1 + \sum_1^{b-1} \psi_i^2\,(i))\, \sigma_w^2$. (9)
5. Estimate plant output variance σ_y^2 .
6. Calculate index ξ based on the expression
   $\xi = \sigma_y^2 / \sigma_{MV}^2$ (10)

This last step is proposed by [7] as a mean to compare the plant output when the proposed controller is acting with a theoretical plant output using a minimum variance controller.

Frequency Domain Performance Assessment. Kendra[8] proposes a different approach, based on the estimate of the sensitivity transfer function *S(s)* and on the complementary sensitivity transfer function *T(s)*. Considering again figure 1, the calculation of those transfer functions can be made. The sensitivity transfer function *S(s)* is obtained as

$$S(s) = (I + G_p(s)\, G_c(s))^{-1} . \quad (11)$$

while complementary sensitivity transfer function *T(s)* is calculated as

$$T(s) = G_p(s)\, G_c(s)\, (I + G_p(s)\, G_c(s))^{-1} . \quad (12)$$

Let the maximum singular value of *S(jw)* be noted as $\underline{\sigma}(S(jw))$. Let the system bandwidth ω_B be the frequency at which $\underline{\sigma}(S(jw))$ becomes greater than $1/\sqrt{2}$. This bandwidth measures the speed at which the system will reject disturbances at the plant output [8].By the same token, $\underline{\sigma}(T(jw))$ can measure the robustness of the controller to uncertainties in the plant model used to design the controller.

Bearingless Motor Prototype Modeling

The prototype available at the Laboratory of Applied Superconductivity (LASUP), at the Federal University of Rio de Janeiro (UFRJ) is a two phase four pole split winding bearingless induction machine [3,4]. Figure 2 show its geometry and winding arrangement.

Though the prototype has been constructed to have one axial bearing based on super-conductive material, and two sets of radial bearings, one upper and one lower, presently the axial bearing and the lower radial bearings set have been replaced by mechanical devices, while the upper bearing is still magnetic. This simplified structure was used in [4], where the plant dynamics was modeled, and a control scheme based on LQR algorithm was obtained.

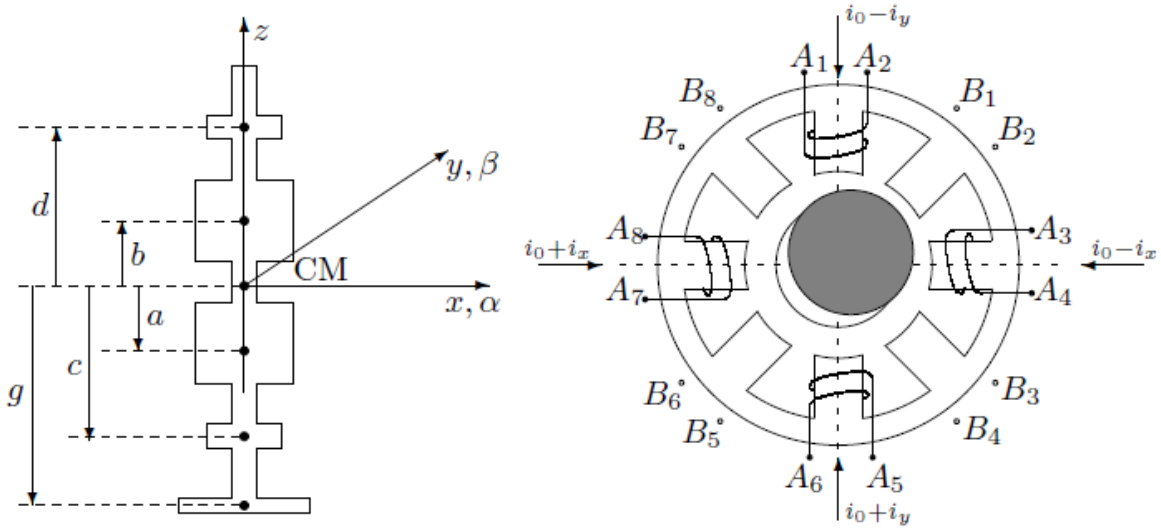

Figure 2 Rotor geometry and stator windings

The same prototype was used by [3], with a decentralized PID control. According to the modeling in [4], the basic rotor dynamic equation is:

$$J_0\,\ddot{\mathbf{z}}(t) + G_r\dot{\mathbf{z}}(t) = \mathbf{e}_r(t). \qquad (13)$$

Where the inertia matrix J_0, the gyroscopic matrix G_r, and the angular coordinates vector $\mathbf{z}$ and the external excitation vector $\mathbf{e_r}$ are given by

$$J_0 = \begin{bmatrix} J & 0 \\ 0 & J \end{bmatrix} \quad ; \quad G_r = \begin{bmatrix} 0 & \omega_r I_z \\ -\omega_r I_z & 0 \end{bmatrix} \quad ; \quad \mathbf{z} = \begin{bmatrix} \beta \\ -\alpha \end{bmatrix} \quad ; \quad \mathbf{e}_r = \begin{bmatrix} \sum p_y \\ \sum -p_x \end{bmatrix}.$$

The moments of inertia of the rotor are $I_x = I_y = I$ and I_z; if m is its mass, then $J = J_x = J_y = I + m\,c^2$. The rotational speed is ω_r and $p_{x,y}$ are the external torques applied. Since α and β are usually small, the angular coordinates in $\boldsymbol{z}$ can be replaced by the displacements at the sensor level, $\boldsymbol{z_s} = [x_d \quad y_d]^T$, resulting in the following equation.

$$\ddot{\boldsymbol{z}}_s(t) + G_{rr}\dot{\boldsymbol{z}}_s(t) + (\gamma_{rr} - K^r_{zr})\boldsymbol{z}_s(t) = K^r_{ur}\,\boldsymbol{u}(t). \qquad (14)$$

where the input vector $\boldsymbol{u} = [i_x \quad i_y]^T$ stores the control currents imposed on the x and y directions. The matrix coefficients are:

$$G_{rr} = J_0^{-1} \quad ; \quad \gamma_{rr} = J_0^{-1}\,m\,\gamma\,c \quad ; \quad K^r_{zr} = J_0^{-1}\,2\,K_{pb}\,(b-c) \; ; \quad K^r_{ur} = J_0^{-1}\,(d-c)(b-c)$$

where the constants K_{pb} and K_{ib} represent the linearization of the eletromagnetic restoring force due to gap variations and excitation currents applied to the magnetic bearing, being γ the gravity acceleration. Equation (14) can be written as a first order linear system by re-definition of the variables, as

$$\boldsymbol{x} = [\boldsymbol{z_s} \quad \dot{\boldsymbol{z}}_s]^T = [x_d \quad y_d \quad \dot{x}_d \quad \dot{y}_d]^T. \qquad (15)$$

resulting in

$$\dot{\boldsymbol{x}}(t) = \begin{bmatrix} 0 & I \\ A_{z1} & A_{z2} \end{bmatrix}\boldsymbol{x}(t) + \begin{bmatrix} 0 \\ B_z \end{bmatrix}\boldsymbol{u}(t) \qquad (16)$$

The blocks in the *A* and *B* matrices above are all 2 x 2 with $A_{21} = K_{zr} - \gamma_{rr}$, $A_{22} = -G_{rr}$ and $B_2 = K_{ur}$.

Controller Performance – Simulations

Using the LASUP prototype parameters in the model presented above, and considering a frequency of 120 Hz applied to the windings of the bearingless motor, the following values are obtained for equation (16):

$$A_{21} = 344765 \begin{bmatrix} 1 & 0 \\ 0 & 1 \end{bmatrix} \; ; \; A_{22} = \begin{bmatrix} 0 & -40.9 \\ 40.3 & 0 \end{bmatrix} \; ; \; B_2 = 78.6 \begin{bmatrix} 1 & 0 \\ 0 & 1 \end{bmatrix}$$

Two control laws were applied: a state feedback ($\boldsymbol{u} = F_c \, \boldsymbol{x}$) centralized LQR, and a decentralized PID control. The LQR control structure was obtained using MATLAB lqr(.) algorithm, resulting in the following feedback matrix F:

$$F_c = \begin{bmatrix} -8777 & -6.852 & -78.89 & 0 \\ -6.852 & -8777 & 0 & -78.89 \end{bmatrix} \qquad (17)$$

In the decentralized PID scheme, each direction *x* and *y* was treated as an independent channel; it used a Simulink PID control block, with a compensator to implement derivative action, in order to avoid amplifying noise. PID parameters were chosen to obtain stability, without much consideration on performance characteristics. PID parameters are listed in table 1. Both approaches were simulated, using Simulink.

Table 1 PID parameter values

Parameter	Parameter value
Proportional gain	5000
Integral gain[sec^{-1}]	10
Derivative gain[sec]	10
Derivative divider	100

Stochastic Performance Evaluation. The LQR controller was simulated for a 1 second, with a sampling rate of 1 kHz. The time series obtained was fed to the *armax(.)* function of MATLAB and the models obtained for channels *x* and *y* are shown on table 2. It should be remarked that noise variance is also generated by this same *armax(.)* function.

Table 2 ARMA models for system outputs

Controller	Channel	$G(z^{-1})$
LQR	X	$\frac{1 - 1.829\,z^{-1} + 0.8293\,z^{-2}}{1 - 2.731\,z^{-1} + 2.503\,z^{-2} - 0.7705\,z^{-3}}$
	Y	$\frac{1 - 1.626\,z^{-1} + 0.9284\,z^{-2}}{1 - 2.357\,z^{-1} + 2.013\,z^{-2} - 0.6062\,z^{-3}}$
PID	X	$\frac{1 - z^{-1}}{1 - 2.828\,z^{-1} + 2.775\,z^{-2} - 0.9436\,z^{-3}}$
	Y	$\frac{1 - z^{-1}}{1 - 2.786\,z^{-1} + 2.669\,z^{-2} - 0.9045\,z^{-3}}$

Following [6], the impulse response is obtained from the ARMA transfer function by continued division, resulting in the functions shown in table 3. The variances for *x* and *y* were then calculated using MATLAB function *var(.)*. Table 4 shows both noise variance and output variances. Using expressions (9) and (10), σ_{MV}^2 and ξ were calculated. Those results

are also displayed in table 4. The same procedure described above, was applied to the control scheme using decentralized PID controllers, resulting in the following data displayed on tables 2, 3 and 4.

Table 3 Impulse response

Controller	Loop	$\psi(z^{-1})$
LQR	X	$1+.902\,z^{-1}+.790\,z^{-2}+.669\,z^{-3}+\cdots$
	Y	$1+.731\,z^{-1}+.638\,z^{-2}+.639\,z^{-3}+\cdots$
PID	X	$1+1.828\,z^{-1}+2.394\,z^{-2}+2.642\,z^{-3}+\cdots$
	Y	$1+1.786\,z^{-1}+2.276\,z^{-2}+2.427\,z^{-3}+\cdots$

Table 4 Noise and output variances, performance indexes

Controller	Loop	White noise variance	Output variance	σ_{MV}^2	ξ
LQR	X	4.3466e-012	1.8655e-011	4.35E-12	4.2885
	Y	4.5369e-012	1.8844e-011	6.96E-12	2.7075
PID	X	1.7521e-010	2.731e-08	7.61E-10	35.887
	Y	1.8941e-010	2.7563e-08	1.78E-09	2.7075

By comparing the data shown on table 4, it is noticeable that the performance of the LQR controller , for this specific plant dynamic, is better than the PID approach, at least for *x*, since performance index is almost a decade smaller for the LQR case.

Frequency Domain Performance Evaluation. Based on [8], the plant model is driven by pseudo random noise, applied to each input at a time; the time series obtained for *x* and *y* are submitted to MATLAB *oe()*, as suggested in [8], in order to obtain the sensitivity transfer function S. For the LQR controller applied to the bearingless motor model, the following matrix S was reached:

$$S_{LQR}=\begin{bmatrix}\dfrac{-1+1.054z^{-1}}{1-0.9617z^{-1}+0.01543z^{-2}} & \dfrac{-5.378.10^{-6}+1.024.10^{-5}z^{-1}}{1-1.886z^{-1}+0.8895z^{-2}}\\ \dfrac{-5.378.10^{-6}+1.024.10^{-5}z^{-1}}{1-1.886z^{-1}+0.8895z^{-2}} & \dfrac{-1+1.054z^{-1}}{1-0.9617z^{-1}+0.01543z^{-2}}\end{bmatrix}. \quad (18)$$

This sensitivity matrix was submitted to MATLAB function sigma(.) in order to calculate the singular values. Figure 3a shows the frequency response obtained. It should be noted that the peak value is 0.6 dB for a frequency of 400 rd/s, indicating a reasonable disturbance rejection figure. The same procedure was applied to the PID controller, resulting in the frequency response shown in figure 3b for the singular value of the PID sensitivity transfer function. The peak value obtained is 45 dB at a frequency of 350 rd/s, indicating a low disturbance rejection figure.

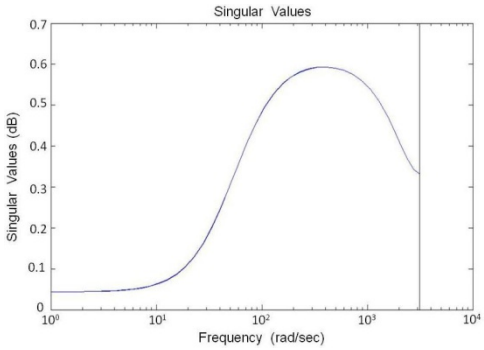

Figure 3a $\underline{\sigma}(S)$ for LQR controller

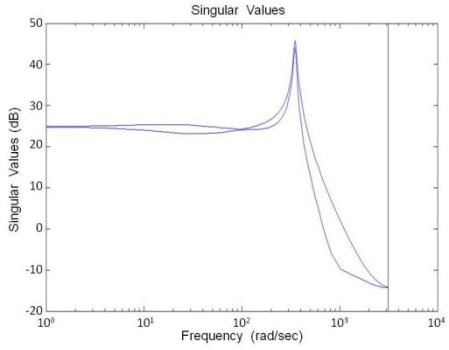

Figure 3b $\underline{\sigma}(S)$ for PID controller

Controller Performance – Experimental Data

In order to check simulations results with experimental data, the bearingless motor prototype was used to produce time series, with LQR and PID controllers. For this experimental tests only the time domain performance evaluation was applied. The time series obtained was fed to MATLAB generating models developed for channels *x* and *y*. The impulse response was obtained from the ARMA transfer function, resulting in the functions shown in table 5.

Table 5 Impulse response

Controller	Loop	$\psi(z^{-1})$
LQR	X	$1 + 1.519\,z^{-1} + 1.625\,z^{-2} + 1.498\,z^{-3} + \cdots$
	Y	$1 + 1.743z^{-1} + 2.093\,z^{-2} + 2.157z^{-3} + \cdots$
PID	X	$1 + 1.454z^{-1} + 1.806z^{-2} + 1.846z^{-3} + \cdots$
	Y	$1 + 1.742z^{-1} + 2.331z^{-2} + 2.571z^{-3} + \cdots$

These results suggest that a delay b =2 should be considered. Finally, using expressions (9) and (10), σ_{MV}^2 and ξ were calculated. The same procedure described above, was applied to the control scheme using decentralized PID controllers, resulting in the data shown on table 6.

Table 6 Performance index

Controller	Loop	σ_{MV}^2	ξ
LQR	X	0.0063	3.627
	Y	0.00087	6.233
PID	X	0.0072	6.299
	Y	0.0033	10.69

By comparing the resulting performance index shown on table 6, the conclusion is that the performance of the LQR controller, for the real plant, is better than the PID control approach since its performance index is smaller.

Summary

Considering the performance assessment criteria studied, it is clear that, for a real time implementation, the time domain evaluation proposed by [6] and [7] is simpler to be obtained and calculated, since it does not require a testing signal to be injected in the system under evaluation, as well as because the algorithm requires a less sophisticated structure.

References

[1] Schweitzer, G., Maslen, E.H., Editors (2009): Magnetic Bearings. Springer-Verlag, Berlin.
[2] Paiva, J. A., Salazar, A. O., Maitelli, A. L., Stephan, R. M.Performance Improvement of a Split Winding Bearingless Induction Machine Based on a Neural Network Flux Observer In: XI International Symposium on Magnetic Bearings, 2008, Nara.
[3] Gomes, R.R., Stephan, R. M., Santisteban, J. A. Self-Bearing Motor with DSP Based Control System In: X International Symposium on Magnetic Bearings, 2006, Martigny.
[4] Kauss, W. L., Gomes, A. C. N., Stephan, R. M., David, D. LRQ Control of a Bearingless Machine Implemented with a DSP In: XI International Symposium on Magnetic Bearings, 2008, Nara.
[5] Lim, T.M. Zhang D. Control of Lorentz Force-type Self-bearing Motors with Hybrid PID and Robust Model Reference Adaptive Control Scheme. Mechatronics 19 (2008), 35-45
[6] Qin, S.J. Control Performance Monitoring - A Review and Assessment. NSF/NIST Measurement and Control Workshop, New Orleans, March 6-8, 1998.
[7] Harris, T.J., Seppala, C.T., Desborough, L.D.: A Review of Performance Monitoring and Assessment Techniques for Univariate and Multivariate Control Systems. Journal of Process Control 9 (1999) 1-17. Elsevier.
[8] Kendra, S.J., Çinar, A.: Controller Performance Assessment by Frequency Domain Techniques. J. Process Control, V7 no 3, 181-194 (1997). Elsevier, Great Britain.